

DriveAgent-R1: Advancing VLM-based Autonomous Driving with Hybrid Thinking and Active Perception

Weicheng Zheng^{1,3} Xiaofei Mao² Nanfei Ye²
 Pengxiang Li² Kun Zhan² Xianpeng Lang² Hang Zhao^{1,4*}
¹Shanghai Qi Zhi Institute ²LiAuto ³Tongji University ⁴Tsinghua University

Abstract

Vision-Language Models (VLMs) are advancing autonomous driving, yet their potential is constrained by myopic decision-making and passive perception, limiting reliability in complex environments. We introduce DriveAgent-R1 to tackle these challenges in long-horizon, high-level behavioral decision-making. DriveAgent-R1 features two core innovations: a Hybrid-Thinking framework that adaptively switches between efficient text-based and in-depth tool-based reasoning, and an Active Perception mechanism with a vision toolkit to proactively resolve uncertainties, thereby balancing decision-making efficiency and reliability. The agent is trained using a novel, three-stage progressive reinforcement learning strategy designed to master these hybrid capabilities. Extensive experiments demonstrate that DriveAgent-R1 achieves state-of-the-art performance, outperforming even leading proprietary large multimodal models, such as Claude Sonnet 4. Ablation studies validate our approach and confirm that the agent’s decisions are robustly grounded in actively perceived visual evidence, paving a path toward safer and more intelligent autonomous systems.

Keywords: Autonomous Driving, Vision-Language Models, Hybrid Thinking, Multimodal Chain-of-Thought, Reinforcement Learning

1. Introduction

The paradigm of end-to-end autonomous driving has been substantially advanced by the advent of Vision-Language Models (VLMs) [10, 12, 30, 34, 41], which promise to unify perception, reasoning, and planning into a single, cohesive framework by emulating human-like cognition. This approach holds the potential for superior generalization and a deeper understanding of complex scenarios. However, to achieve truly reliable autonomous driving, an agent must possess not only comprehension but also foresight and proactivity. In the context of motion planning, the task can be decon-

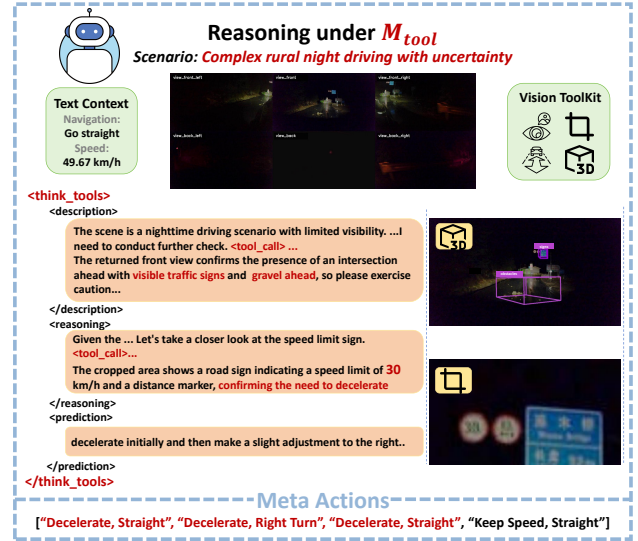


Figure 1. An illustration of DriveAgent-R1’s reasoning process in a complex nighttime driving scenario with uncertainty. Faced with ambiguity, the agent activates its active perception capabilities, invoking the 3D object detection and RoI inspection tools from its Vision Toolkit to acquire critical visual evidence about an upcoming intersection and a speed limit sign. This new information enables a safer, more grounded decision to decelerate, demonstrating the effectiveness of our Tool-based Multimodal Chain-of-Thought (M-CoT).

*Corresponding at: hangzhao@mail.tsinghua.edu.cn

uncertainty.

Current research, while making significant strides, reveals fundamental limitations in decision-making and perception. In decision-making, while methods like AlphaDrive [13] have pioneered the use of reinforcement learning (RL) to train VLMs for single-step action prediction, they often suffer from myopic decision-making, lacking the capacity for long-term, coherent planning. Regarding perception, a primary obstacle is visual neglect, where in planning tasks, the rich, high-dimensional visual input is often overshadowed by low-dimensional textual commands (e.g., speed, navigation instructions) that provide a more direct signal for the final decision. Although existing works have attempted to mitigate this issue [17, 41], they are still fundamentally characterized by passive perception. They fail to endow agents with the ability to actively seek information as human drivers do, leaving them vulnerable in scenarios with perceptual uncertainty.

Concurrently, the development of Multimodal Chain-of-Thought (M-CoT) [5, 11, 15, 25, 40] offers a promising avenue to enhance the transparency, interpretability, and accuracy of the decision-making process. Its evolution has yielded distinct reasoning patterns, from early forms of Text-based M-CoT [40], which reasons over textual descriptions of the scene, to the more sophisticated, interleaved Tool-based M-CoT [11], which actively invokes tools to gather new visual information mid-reasoning. While the application of such agentic, tool-based reasoning is gaining traction, its use in the specific context of autonomous driving decision-making remains nascent. For instance, concurrent work like AgentThink [27] has demonstrated the value of tool use for visual question answering in driving scenes, but not yet for the planning task itself. The real-world driving environment—a dynamic tapestry of routine situations, and complex long-tail events—presents a unique challenge. Incessantly invoking deliberate, tool-based reasoning in all situations would be computationally excessive and inefficient. A more intelligent approach would be to dynamically adapt the cognitive load, employing efficient Text-based M-CoT for simpler cases and reserving in-depth, Tool-based M-CoT for when the scene’s complexity truly demands it. To our knowledge, such an adaptive mechanism that intelligently integrates different M-CoT modalities for the autonomous driving decision-making task has not yet been explored.

To address these limitations, we introduce *DriveAgent-R1*, an advanced autonomous driving agent engineered for long-horizon, high-level behavioral decision-making. The core of *DriveAgent-R1* is an adaptive Hybrid-Thinking framework, which for the first time enables the agent to dynamically switch between efficient Text-based M-CoT $\mathcal{M}_{\text{text}}$ and in-depth, Tool-based M-CoT $\mathcal{M}_{\text{tool}}$, thereby balancing decision-making efficiency and reliability according to situational demands. Integrated with a powerful Vision Toolkit—which en-

ables on-demand access to high-resolution views and depth maps, among other tools—*DriveAgent-R1* is endowed with active perception, allowing it to proactively resolve perceptual uncertainties (See Fig. 1). Through these innovations, *DriveAgent-R1* systematically overcomes the challenges of myopic decision-making and passive perception, achieving state-of-the-art performance as demonstrated in our extensive experiments.

To cultivate the agent’s hybrid-thinking capabilities, we devise a novel three-stage progressive training strategy centered on RL. Moving beyond the limitations of traditional supervised fine-tuning (SFT), our RL-based approach grants the model the freedom to explore and optimize its own reasoning pathways, which is crucial for mastering the complexities of hybrid thinking. Our strategy begins with SFT to instill foundational knowledge, then proceeds to our proposed Forced-Contrastive Mode Reinforcement Learning (FCM-RL), implemented via a Mode-Partitioned GRPO (MP-GRPO) algorithm, to sharpen the distinct capabilities of each mode. Finally, during Adaptive Mode-Selection Reinforcement Learning (AMS-RL), the agent is trained to autonomously select the optimal thinking mode for any given scenario.

Our main contributions are summarized as follows:

1. We are the first to propose and implement a hybrid-thinking architecture in an autonomous driving agent, *DriveAgent-R1*, which tailors its cognitive mode to the driving scene’s complexity by adaptively switching between Text-based M-CoT and in-depth Tool-based M-CoT.
2. We introduce the concept of active perception to VLM-based driving, empowering the agent with a visual toolkit to significantly enhance its perceptual robustness in uncertain environments.
3. We design a complete, three-stage progressive training strategy centered on RL and establish a comprehensive evaluation suite to assess the model’s performance in prediction accuracy, reasoning quality, and adaptive mode selection.
4. We achieve state-of-the-art performance on the challenging SUP-AD dataset [34], surpassing even larger proprietary VLMs. Furthermore, our ablation studies validate our progressive training strategy and confirm that our agent’s decisions are robustly grounded in visual evidence, paving a validated path toward safer and more intelligent autonomous systems.

2. Related Work

2.1. VLMs for Autonomous Driving

In recent years, VLMs have revolutionized traditional end-to-end autonomous driving by leveraging their powerful capabilities in commonsense reasoning and world knowl-

edge, aiming to unify perception, decision-making, and planning within a single framework. Current explorations primarily unfold along two core directions. The first focuses on enhancing structured reasoning for scene understanding [6, 23, 27, 28, 30]. For instance, DriveLM [30] innovatively employs a Graph Visual Question Answering (GVQA) approach to structure complex driving scenes into logical reasoning graphs, thereby significantly enhancing the model’s zero-shot generalization capabilities in unseen environments. AgentThink [27] introduces “agent-like” dynamic tool use into the question-answering task, enabling the model to bolster its reasoning by proactively validating information. The second core direction concentrates on translating VLM reasoning into actionable driving behaviors, spanning high-level decision-making and low-level planning [13, 17, 20, 34]. In the realm of high-level decision-making, AlphaDrive [13] pioneered the use of GRPO [29] to train a VLM for predicting single-step meta-actions. For low-level motion planning, Drive-R1 [17] identifies that VLMs tend to ignore current visual information and over-rely on historical text. By employing a large-scale domain adaptation strategy to enforce the alignment of visual understanding with trajectory planning, Drive-R1 achieves state-of-the-art performance in trajectory prediction accuracy.

However, despite the significant progress in these works, we argue that existing research exhibits notable limitations in terms of decision foresight and perception proactivity. On one hand, decision-making models like AlphaDrive [13] are often myopic, focusing on single-step intention prediction. On the other hand, while works such as Drive-R1 [17] acknowledge the “visual perception neglect” problem, their solutions primarily rely on static data alignment, lacking the ability to proactively seek information when faced with uncertainty. To address these challenges, we introduce *DriveAgent-R1*, a novel approach that predicts long-horizon driving intentions and incorporates adaptive, active perception. Its core hybrid cognitive framework enables the model to proactively invoke visual reasoning tools when faced with uncertainty, thereby enhancing the robustness and reliability of its decision-making in complex, open-world environments.

2.2. Multimodal Reasoning with Chain-of-Thought

Chain-of-Thought (CoT), a paradigm that guides models to perform step-by-step reasoning, has been proven to significantly enhance the complex reasoning abilities of Large Language Models (LLMs) [7, 37, 39]. Inspired by this, substantial research has been dedicated to extending CoT to the multimodal domain, leading to the formation of M-CoT [9, 18, 22, 36, 40]. Based on how visual information interacts within the reasoning chain, the evolution of M-CoT can be broadly categorized into two main classes [5].

The first class is **Text-based M-CoT**. These methods fol-

low a “perceive then reason” sequential pattern: the VLM first serializes the input image into a textual description, then performs step-by-step reasoning within a pure-text space, leveraging the powerful capabilities of LLMs [16, 40, 44]. However, this approach decouples vision and language interaction, failing to achieve a deeper level of visuolinguistic fusion and potentially losing critical visual details during the initial textual conversion. To better emulate the human cognitive process of “thinking while seeing”, **Interleaved M-CoT** has emerged. This can be further subdivided into two technical paths. One is M-CoT that uses in-process image generation, in which the model creates images mid-reasoning to serve as a “visual scratchpad” [15, 21]. The difficulty lies in the immense demand this places on unifying the model’s ability to both generate and understand visual content simultaneously. Consequently, a more promising and rapidly developing path is **Tool-based M-CoT**. This approach, an embodiment of the model’s agentic capabilities, allows the model to actively invoke external tools to supplement or verify visual information during reasoning [11, 25, 27, 32, 45]. For instance, Visual Sketchpad [11] utilizes a Python graphics library to draw auxiliary lines to aid in geometry problem-solving.

Concurrently, the organizational structure of CoT is another core research direction, mainly divided into unstructured CoT and structured CoT. The former [39] uses simple prompts like “Let’s think step by step” to guide the model in generating free-form natural language reasoning. However, its logical flow and consistency can be difficult to guarantee [19]. To address this, structured CoT aims to standardize the reasoning process through a predefined logical framework [33, 34, 40]. For example, DriveVLM [34] pioneered a three-stage structure of “scene perception → scene analysis → hierarchical planning,” which effectively improved the soundness of its planning.

DriveAgent-R1 integrates and extends the aforementioned research frontiers. It not only adopts the structured CoT paradigm by formulating the reasoning process into three phases—*description*, *reasoning*, and *prediction*—but more centrally, introduces a hybrid-thinking paradigm. This paradigm intelligently combines the efficient Text-based M-CoT with the in-depth Tool-based M-CoT, a design that enables the agent to adaptively switch its reasoning depth within a unified structured framework according to the demands of the driving scenario. Consequently, it strikes a critical balance between decision-making efficiency and reliability.

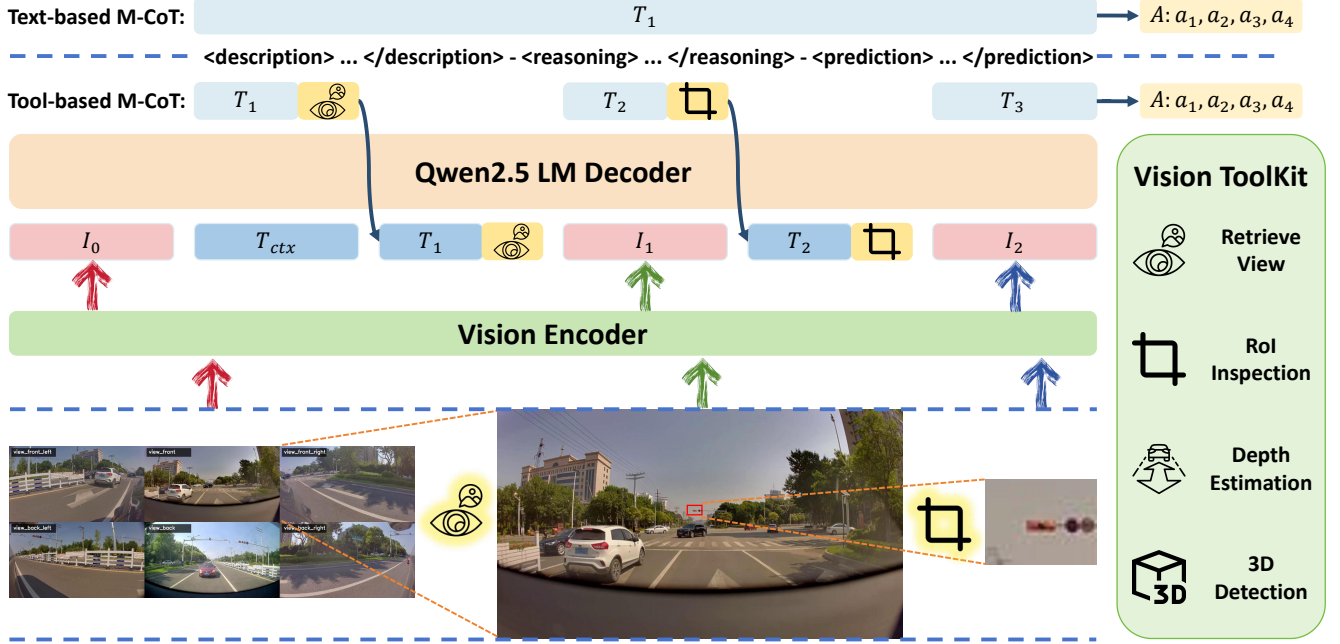


Figure 2. The Hybrid-Thinking architecture of *DriveAgent-RI*. Based on initial visual (I_0) and textual (T_{ctx}) context, the agent selects a reasoning path. **(Top) Text-based M-CoT:** A direct, single-step reasoning path ($T_1 \rightarrow A$) for simple scenarios. **(Bottom) Tool-based M-CoT:** An iterative path for complex scenarios, where the agent interleaves thoughts (T_1, T_2, \dots) with tool calls to acquire new visual evidence (I_1, I_2, \dots), progressively refining its reasoning before generating the final meta-action sequence A .

3. Method

3.1. *DriveAgent-RI*: An Intelligent Driving Agent with Hybrid Thinking

To address the complex and dynamic demands of real-world driving environments, we propose *DriveAgent-RI*, an advanced end-to-end driving decision-making agent featuring a Hybrid-Thinking mechanism. The core concept of this agent is its ability to adaptively select between two distinct thinking modes based on the complexity of the driving scenario. This allows it to strike a critical balance between decision-making efficiency and interpretability, which is paramount in safety-critical domains such as autonomous driving. The hybrid thinking capability of *DriveAgent-RI* is initially established through SFT and subsequently refined and optimized through our novel progressive RL strategy.

3.1.1. Overall Architecture and Problem Formulation

DriveAgent-RI is built upon Qwen2.5-VL-3B [2]. As illustrated in Fig. 2, its architecture comprises a Vision Encoder and a Qwen2.5 Language Model Decoder (LMDecoder). The primary task of the agent is to generate a safe and rational long-horizon driving intention decision based on the multimodal contextual information it receives. The process begins with raw inputs: a set of six synchronized, low-resolution surround-view camera frames and a text string with the current vehicle speed and navigation instructions.

These are processed by their respective encoders. For clarity in our formulation, we denote the resulting tokenized visual embeddings as the Initial visual context I_0 and the textual embeddings as the textual context T_{ctx} . Based on these inputs, the agent outputs a meta-action sequence A , which describes the driving intention for the next 8 seconds. This sequence is composed of four discrete meta-actions, each with a 2-second timestep: $A = (a_1, a_2, a_3, a_4)$. Each meta-action $a_t = (s_t, j_t)$ consists of a velocity token s_t from the velocity vocabulary $V_s = \{\text{Accelerate, Keep Speed, Decelerate, Stop}\}$ and a trajectory token j_t from the trajectory vocabulary $V_j = \{\text{Straight, Right Turn, Left Turn}\}$.

3.1.2. Hybrid-Thinking Process

Given an input (I_0, T_{ctx}) , *DriveAgent-RI* first generates a special token to determine which reasoning path to follow. Crucially, regardless of the chosen mode, its entire thinking process adheres to a unified, structured three-stage chain-of-thought framework: *description*, *reasoning*, and *prediction*. This framework serves as the foundation for all its decisions, where the *description* stage involves initial perception of the scene, the *reasoning* stage conducts logical and causal analysis, and finally, the *prediction* stage summarizes the analysis to determine the driving intent.

The two thinking modes are primarily distinguished by their form of reasoning.

Text-based M-CoT (\mathcal{M}_{text}) For the majority of common

driving scenarios where effective decisions can be made relying solely on the default low-resolution visual information and textual context, *DriveAgent-RI* generates the `<think_text>` token, activating the $\mathcal{M}_{\text{text}}$ mode. In this mode, the agent relies entirely on its internal knowledge and the initial input (I_0, T_{ctx}) to make decisions through pure text-based reasoning within the three-stage framework. Its primary advantage is computational efficiency, which makes it the appropriate choice for routine scenarios where the available information is adequate, thereby obviating the need for tool-based perceptual enhancement.

Tool-based M-CoT ($\mathcal{M}_{\text{tool}}$) In complex or uncertain scenarios where the initial visual context is insufficient for reliable decision-making, *DriveAgent-RI* generates the `<think_tool>` token, activating the $\mathcal{M}_{\text{tool}}$ mode. In this mode, the agent actively invokes external visual tools to acquire additional information, enriching and deepening the three-stage thinking process in an interleaved, multimodal fashion. The tool calls and their returned information are seamlessly embedded within any stage of the structured chain of thought. For instance, the model might call a tool during the *description* stage to get a clearer view or during the *reasoning* phase to verify a driving hypothesis. This dynamic, iterative process can be formalized as a state transition system. Let H_k denote the contextual history after the k -th interaction. The evolution of the agent’s reasoning process is governed by the following recurrence:

$$H_{k+1} = H_k \oplus T_k \oplus I_{k+1}, \quad \text{for } k < K$$

where $(T_k, \mathcal{T}_{k+1}) = \text{LMDecoder}(H_k)$ and $I_{k+1} = \text{VisionEncoder}(\text{Execute}(\mathcal{T}_{k+1}))$. The process begins with an initial history $H_0 = I_0 \oplus T_{\text{ctx}}$, where \oplus denotes the concatenation operator. In each step k , *DriveAgent-RI* generates reasoning text token T_k and potentially a tool call request \mathcal{T}_{k+1} based on its current history H_k . If a tool is called, the system executes it to obtain new raw visual information, which is then encoded into an image embedding I_{k+1} and integrated into the history. This interleaving process, visually represented in Fig. 2, continues until *DriveAgent-RI* either generates the final meta-action sequence A without a subsequent tool call, or reaches a predefined maximum number of interaction K . This mode significantly enhances the agent’s ability to handle complex scenarios and improves the interpretability of its decision-making process.

3.1.3. Active Perception and Vision Toolkit

DriveAgent-RI is integrated with a powerful suite of visual tools, endowing it with the capability of Active Perception. These tools allow the model to explore the environment on-demand during its reasoning process to acquire critical information.

Retrieve High-Resolution View. This tool allows the agent to request the original high-resolution image from

any specific viewpoint. Its design is motivated by human drivers who consciously check specific mirrors or windows to get a clear view of the road conditions before critical maneuvers like lane changes or turns. More importantly, this tool incorporates a **Historical Memory Pool**, which caches images from all viewpoints over the past 5 seconds, sampled at 1Hz. This enables the model to intelligently look back at historical frames to assess changes in traffic light status or the movement trends of dynamic objects, thus avoiding the high computational cost and latency associated with processing redundant information from full video sequences.

RoI Inspection. This tool empowers the agent with a “zoom-in” capability for meticulous examination of critical areas. Based on any high-resolution view, the agent can request to crop and magnify a specific **Region of Interest (RoI)** by providing the absolute pixel coordinates of its bounding box. This is not merely a passive utility; it is a direct manifestation of the model’s Inherent Localization Ability. This allows for fine-grained analysis and focused viewing of any region the agent deems important, which is vital for confirming details such as the status of distant traffic lights or the text on traffic signs.

Depth Estimation. Accurately perceiving the 3D spatial relationship between the ego-vehicle and other traffic participants (e.g., vehicles, pedestrians) is fundamental to safe driving. This tool leverages the state-of-the-art monocular depth estimation algorithm, Depth Anything V2 [42], to generate a depth map for a specified view. The resulting depth map provides rich geometric information, enabling the model to intuitively grasp the relative distances and spatial layout of objects, as well as the overall road structure, which is crucial for path planning and obstacle avoidance.

3D Object Detection. To comprehensively understand the dynamic environment, the agent must identify key objects and ascertain their precise 3D spatial information (position, size, and orientation). We integrate an advanced open-vocabulary, single-monocular 3D object detection tool that works with arbitrary camera views [43]. This tool not only detects a predefined set of common objects like cars, pedestrians, and traffic signs but its “open-vocabulary” nature also allows the model to dynamically specify new objects for detection based on the current scene’s needs, demonstrating remarkable flexibility and adaptability. The output from this tool provides indispensable input for subsequent trajectory prediction and risk assessment.

3.2. Progressive Training Strategy for Hybrid-Thinking

To cultivate the hybrid-thinking capabilities of *DriveAgent-RI*, we devise a progressive, three-stage training strategy. This strategy, through a phased approach of “foundation building \rightarrow mode strengthening \rightarrow autonomous decision-making,” aims to systematically address the core challenges

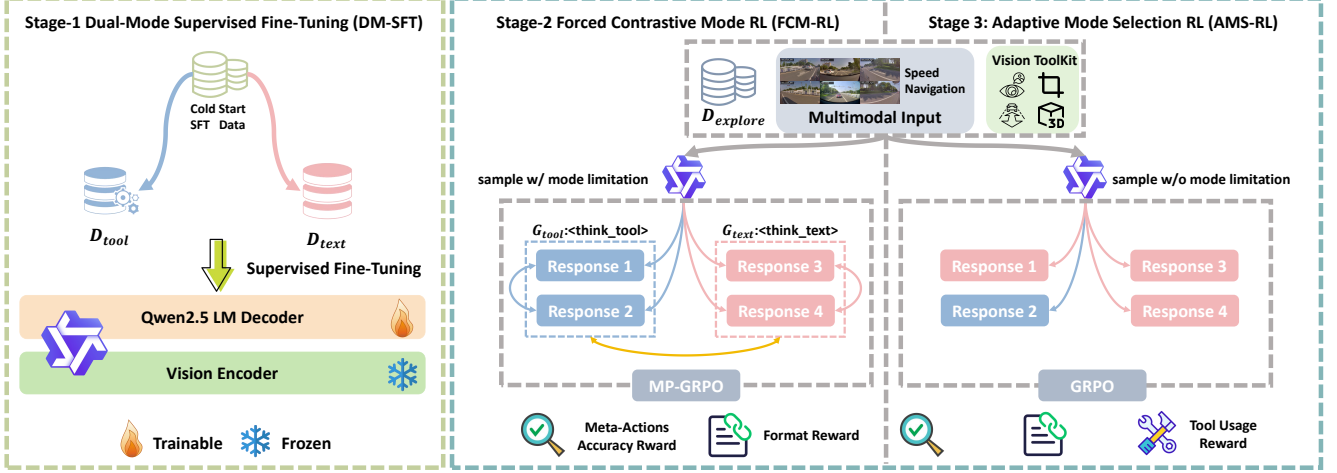


Figure 3. The progressive three-stage training strategy for *DriveAgent-RI*. This strategy systematically develops hybrid-thinking capabilities. (Stage 1) DM-SFT: The language model decoder is first fine-tuned on a dual-mode dataset to build a foundational understanding of both text-based and tool-based reasoning. (Stage 2) FCM-RL: We then use MP-GRPO to strengthen each mode. The agent is forced to generate responses in both modes for each input, creating a contrastive signal that improves performance in each paradigm. (Stage 3) AMS-RL: Finally, the agent learns to autonomously select the optimal mode. Using the standard GRPO algorithm, it is trained without mode forcing, guided by a new reward that specifically encourages effective tool usage.

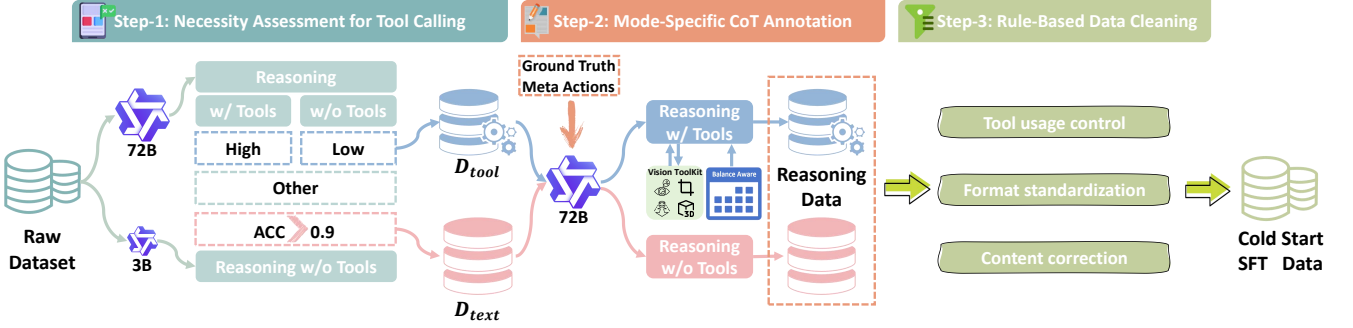


Figure 4. The automated data construction pipeline for our cold-start SFT. The pipeline consists of three steps: (1) Necessity Assessment for Tool Calling, which partitions the raw data into tool-necessary (D_{tool}) and tool-unnecessary (D_{text}) sets using 3B and 72B models; (2) Mode-Specific CoT Annotation, where a 72B teacher model generates reasoning steps via inverse reasoning from ground-truth meta actions; and (3) Rule-Based Data Cleaning, which ensures the final quality of the SFT dataset.

in mastering hybrid-thinking capabilities. These challenges range from understanding the logic and timing of tool calls, to mastering the distinct paradigms of text-based \mathcal{M}_{text} and tool-based \mathcal{M}_{tool} reasoning, and ultimately, to achieving adaptive selection of the most efficient and reliable thinking mode based on the scenario.

3.2.1. Stage 1: Dual-Mode Supervised Fine-Tuning

We begin by cold-starting the model using SFT. The primary objective of this stage is to endow *DriveAgent-RI* with a foundational understanding of the format and semantic boundaries of the two thinking modes.

Cold-Start Data Construction Pipeline

To provide high-quality data for the SFT phase, we propose an automated data construction pipeline structured as a

three-stage workflow (Fig. 4). This pipeline systematically processes raw datasets - which exclusively contain multi-modal inputs and ground-truth meta-actions - and converts them into comprehensive reasoning datasets that effectively integrate both \mathcal{M}_{tool} and \mathcal{M}_{text} reasoning modalities.

Step 1: Necessity Assessment for Tool Calling

This initial step partitions the raw dataset by discerning the necessity of tool use for each sample. Our two-model approach aims to establish clear boundaries for scenario complexity. We first employ a lightweight Qwen2.5-VL-3B model to filter out simple scenarios where high accuracy is achievable in the \mathcal{M}_{text} mode, forming the tool-unnecessary set D_{text} . For the remaining samples, a powerful Qwen2.5-VL-72B oracle model determines the tool-necessary set D_{tool} by identifying cases where the \mathcal{M}_{tool} mode yields a signif-

icant performance gain over the $\mathcal{M}_{\text{text}}$ mode. This use of a highly capable oracle provides a reliable, conservative criterion for tool necessity, ensuring that we identify scenarios where external perception is genuinely beneficial, while leaving ambiguous cases for the exploratory set D_{explore} used in subsequent RL stages.

Step 2: Mode-Specific CoT Annotation

In this step, we generate mode-specific CoT annotations using the powerful Qwen2.5-VL-72B as the “teacher model.” For each classified sample, the teacher model performs “inverse” reasoning from the ground-truth meta-actions to construct a logical thought process in either the $\mathcal{M}_{\text{text}}$ or $\mathcal{M}_{\text{tool}}$ mode. To ensure a balanced distribution of tool use within the D_{tool} set, a **Dynamic Tool Preference Guidance mechanism** is employed during this process, preventing a preference bias in the annotated data.

Step 3: Rule-Based Data Cleaning

In the final step, the annotated data is subjected to a rule-based cleaning pipeline to ensure its fidelity and uniformity. This pipeline validates the structural integrity of the CoT and the syntactical correctness of tool calls, rectifies content-level errors such as annotation artifacts or prediction-label mismatches, and normalizes tool usage by constraining call frequency and eliminating redundancies.

After this pipeline, we sample an equal number of high-quality instances from D_{text} and D_{tool} to construct the final cold-start SFT dataset for building the foundational hybrid-thinking capabilities of the model.

3.2.2. Stage 2: Forced Contrastive Mode Reinforcement Learning

Following the initial SFT stage, *DriveAgent-RI* possesses a basic understanding of both thinking modes. The objective of this stage is to strengthen and deepen the agent’s independent performance in each mode. We employ RL to further unlock the model’s potential, ensuring that it does not develop a bias against a mode due to initially weaker performance when it later needs to make autonomous decisions (e.g., prematurely abandoning the $\mathcal{M}_{\text{tool}}$ mode, thus precluding any opportunity for improvement).

To this end, we adapt the GRPO [29] algorithm, which has proven effective in multimodal reasoning and autonomous driving [13, 18, 32, 45], proposing a variant we term **Mode-Partitioned GRPO (MP-GRPO)**. As shown in Fig. 3, for each input from D_{explore} , we compel the agent to generate two mode-specific groups of responses, G_{text} and G_{tool} , by forcing the corresponding mode token (`<think_text>` or `<think_tool>`) in the prompt. All responses from both groups are then aggregated into a global set for reward normalization and advantage calculation. The key advantage of this design is the creation of a **multi-dimensional contrastive learning signal**: it facilitates not only **intra-mode** comparison between different response trajectories but also **inter-mode** comparison. This multi-faceted contrast allows

the agent to simultaneously enhance its specific capabilities in both modes and gain an initial understanding of the suitability of each mode for different scenarios, laying a critical foundation for the final stage of adaptive selection.

Reward Design. The agent’s learning is guided by an outcome-driven reward function that evaluates the entire reasoning trajectory. This reward is a composite of two key components: an accuracy reward (R_{acc}) and a format consistency reward (R_{fmt}), formulated as follows:

$$R = R_{\text{acc}} + w_{\text{fmt}} \cdot R_{\text{fmt}},$$

where the accuracy reward R_{acc} is a weighted average of similarity scores for the predicted speed and trajectory sequences. To account for the diversity of valid driving decisions, the core similarity function robustly evaluates both strict sequence matching and broader action trends (see Appendix for formulation details). The format consistency reward R_{fmt} is a rule-based score that penalizes structural errors and, more critically, action-declaration inconsistency, such as invoking tools in the $\mathcal{M}_{\text{text}}$ mode or failing to do so in the $\mathcal{M}_{\text{tool}}$ mode. This forces the agent to learn the distinct boundaries of each thinking mode.

3.2.3. Stage 3: Adaptive Mode Selection Reinforcement Learning

After the foundational and contrastive learning in the first two stages, *DriveAgent-RI* is proficient at generating high-quality reasoning within both modes independently. This final stage focuses on achieving true hybrid thinking: training the agent to autonomously select the optimal thinking mode based on the context. To achieve this, we remove the mode-forcing constraints of Stage 2 and employ the native GRPO algorithm. The agent must now autonomously generate the initial mode-selection token (`<think_text>` or `<think_tool>`) and proceed with the corresponding reasoning path.

Reward Design. To guide this learning process, the reward function is augmented with a conditional tool-usage reward, R_{tool} , which encourages the effective and judicious use of tools only when the $\mathcal{M}_{\text{tool}}$ mode is chosen. The total reward is defined as:

$$R = R_{\text{acc}} + w_{\text{fmt}} \cdot R_{\text{fmt}} + \mathbb{I}(\text{mode} = \mathcal{M}_{\text{tool}}) \cdot R_{\text{tool}},$$

where the definitions of R_{acc} and R_{fmt} remain consistent with Stage 2. The core of R_{tool} is a dynamic reward mechanism based on curriculum learning [3], designed to incentivize meaningful tool use. This mechanism evaluates the effectiveness of a tool-use trajectory by comparing its final accuracy against a dynamic reward window that becomes progressively stricter during training. Trajectories that lead to high accuracy are rewarded, while ineffective ones are penalized, encouraging exploration in early training phases

and demanding high-precision, impactful tool use in later stages.

Through these three interconnected and progressive training stages, *DriveAgent-RL* not only masters the execution of two distinct thinking modes but, more importantly, learns to autonomously and rationally choose between them based on the complexity and uncertainty of the driving scenario, thereby achieving robust, efficient, and interpretable hybrid-thinking decisions.

4. Experiments

4.1. Setup

4.1.1. Dataset

All our experiments are conducted on the SUP-AD dataset [34]. This dataset is meticulously curated with a focus on long-tail and challenging scenarios, covering over 40 diverse driving situations such as road construction and animal crossings. It comprises 35K video clips, with a single keyframe selected from each as a sample. We randomly partition 1,500 samples from the dataset to form our test set. For the training data, we first process the remaining data using the construction pipeline described in Section 3.2.1. For Stage 1 (DM-SFT), we filter, annotate, and clean 5K high-quality samples, equally split between the tool-necessary set D_{tool} and the tool-unnecessary set D_{text} (2.5K each). During the annotation process, our tool-balancing guidance strategy ensures that the four tool types have an approximately equal usage distribution of 25% each. For the RL in Stage 2 and Stage 3, we utilize the exploratory set D_{explore} , which consists of samples not assigned to the other sets during the first step of our data pipeline.

4.1.2. Evaluation Metrics

To comprehensively evaluate the model’s performance, we designed a suite of metrics across three dimensions:

Accuracy (ACC). To assess the precision of the agent’s high-level decision-making, we compute both First-Frame and Sequence Average Joint Accuracy. For a prediction to be considered correct, the composite meta-action (both speed and trajectory) must exactly match the ground truth. To encourage safer, more conservative predictions, we incorporate a Relaxed Speed Matching mechanism, which awards a full score for an exact match and partial scores of 0.5 and 0.2 for predictions that are one and two levels safer than the ground truth, respectively.

Holistic Evaluation Score (H-Score). As rule-based ACC cannot assess reasoning quality or the diversity of valid decisions, we introduce the Holistic Evaluation Score (H-Score). This metric uses a state-of-the-art large model as an evaluator to provide a comprehensive score for both the reasoning process and the predicted sequence based on *safety*, *comfort*, and *accuracy*. To ensure a fair comparison, scores

are normalized against the ground-truth performance on each sample.

Mode Selection Accuracy (MSA). To quantify the ability of *DriveAgent-RL* to dynamically select the appropriate thinking mode, inspired by [14], we propose the Mode Selection Accuracy metric. For each sample x_i in the test set, we run our model under three conditions: forced $\mathcal{M}_{\text{tool}}$ mode, forced $\mathcal{M}_{\text{text}}$ mode, and free-choice mode. First, we define the optimal thinking mode m_i^* for sample x_i . Let $\text{Acc}(x_i, m)$ be the accuracy achieved when forced to use mode m . The optimal mode is defined as:

$$m_i^* = \begin{cases} \mathcal{M}_{\text{tool}} & \text{if } \text{Acc}(x_i, \mathcal{M}_{\text{tool}}) > \text{Acc}(x_i, \mathcal{M}_{\text{text}}) \\ \mathcal{M}_{\text{text}} & \text{otherwise} \end{cases}$$

This definition selects the mode with higher accuracy, defaulting to the more efficient $\mathcal{M}_{\text{text}}$ mode in case of a tie. Let $m_{\text{free}}(x_i)$ be the mode the agent actually selects in the free-choice setting. The MSA is then the proportion of samples for which the agent makes the optimal choice:

$$\text{MSA} = \frac{1}{N} \sum_{i=1}^N \mathbb{I}(m_{\text{free}}(x_i) = m_i^*),$$

where N is the total number of test samples and $\mathbb{I}(\cdot)$ is the indicator function.

4.1.3. Implementation Details

We use Qwen2.5-VL-3B [2], a compact yet powerful open-source Vision-Language Model, as the backbone for our agent. All training is conducted on 8 H20 GPUs. For all multimodal inputs in our experiments, the maximum number of pixels per image is set to 259,200. During RL stages, the maximum number of tool calls allowed per trajectory is 3. For SFT (Stage 1), we fine-tune the model for 78 iterations with a learning rate of 2.0×10^{-5} and a batch size of 256, keeping the vision encoder frozen. The subsequent RL stages (Stage 2 & 3) employ the GRPO framework with an overall group size of 4. Specifically, Stage 2 utilizes our proposed MP-GRPO algorithm, where each of the two mode-specific groups ($\mathcal{M}_{\text{text}}$ and $\mathcal{M}_{\text{tool}}$) contains 2 samples. A cosine annealing learning rate schedule is used for all training stages.

4.2. Main results

To comprehensively evaluate the performance of our proposed *DriveAgent-RL*, we benchmark it against its base model (Qwen2.5-VL-3B) and a suite of state-of-the-art (SOTA) VLMs. As detailed in Table 1, we report the performance of all models under two distinct settings: one where the agent is forced to rely on text-based reasoning (w/o Tools), and another where it is free to invoke visual tools (w/ Tools). Our results yield several key insights.

Tool-Use Enhances SOTA VLMs’ Capabilities. Our primary finding is that access to the vision toolkit generally

Table 1. **Comparing *DriveAgent-RL* with baseline and state-of-the-art VLMs.** The baseline and SOTA VLMs are evaluated in a one-shot manner, where tool-use is enabled via prompting without any training. We report performance under two settings: without our proposed visual tools (*w/o Tools*), which forces the agent into the $\mathcal{M}_{\text{text}}$ mode, and with tools enabled (*w/ Tools*), which allows the agent to choose its reasoning mode between $\mathcal{M}_{\text{text}}$ and $\mathcal{M}_{\text{tool}}$. The percentage change relative to the ‘w/o Tools’ setting is shown in parentheses (blue for improvement, red for degradation). Best results are highlighted in **bold**. \uparrow indicates that higher is better.

Model	First Frame Acc. (%) \uparrow		Sequence Avg. Acc. (%) \uparrow		H-Score (by Gemini 2.5 Pro [8]) \uparrow			
	Joint		Joint		Prediction		Reasoning	
	w/o Tools	w/ Tools	w/o Tools	w/ Tools	w/o Tools	w/ Tools	w/o Tools	w/ Tools
<i>Baselines (one-shot Prompting)</i>								
Qwen2.5-VL-3B [2]	16.28	9.42 (-42.1%)	19.41	10.86 (-44.0%)	4.06	3.64 (-10.3%)	2.38	1.87 (-21.4%)
<i>State-of-the-Art VLMs (one-shot Prompting)</i>								
Qwen-VL-Max-Latest [2]	23.99	25.53 (+6.4%)	34.37	34.57 (+0.6%)	5.68	6.31 (+11.1%)	5.15	6.18 (+20.0%)
Doubao-Seed-1.6 [4]	29.03	32.82 (+13.1%)	34.77	36.94 (+6.2%)	6.49	7.07 (+9.1%)	6.30	7.26 (+15.2%)
Claude Sonnet 4 [1]	24.02	30.03 (+25.0%)	33.37	35.34 (+5.9%)	5.83	6.60 (+13.2%)	5.55	7.00 (+26.1%)
Gemini 2.5 Flash [8]	36.51	36.22 (-0.8%)	38.54	38.91 (+1.0%)	8.00	7.80 (-2.5%)	8.22	8.37 (+1.8%)
GPT-4.1 [24]	31.20	31.88 (+2.2%)	36.27	37.06 (+2.2%)	8.10	7.67 (-5.3%)	7.90	7.80 (-1.3%)
<i>Our Method</i>								
DriveAgent-RL (Ours)	61.42	70.11 (+14.2%)	38.03	44.06 (+15.9%)	7.68	8.39 (+9.2%)	7.16	8.00 (+11.7%)

enhances the decision-making of SOTA VLMs. For example, when given access to tools, Claude Sonnet 4 achieves a 25.0% increase in joint accuracy and a 26.1% boost in reasoning quality. This provides strong evidence that proactively acquiring visual information is a promising direction for improving VLM-based driving agents.

The Double-Edged Sword of Visual Tools. Visual tools can be a double-edged sword. Our experiments show that when the baseline Qwen2.5-VL-3B model is granted tool access without specialized training, its performance collapses, suffering a 42.1% drop in joint accuracy. This critically highlights that tools only become an asset for autonomous planning when the agent is explicitly trained to leverage them; otherwise, they can disrupt the model’s reasoning by introducing uncertainty, thus becoming a liability.

DriveAgent-RL: From Distraction to Amplifier. In stark contrast, *DriveAgent-RL* successfully learns to leverage the visual toolkit through our progressive training strategy. Unlike its base model, our agent demonstrates significant improvements across all metrics when tools are enabled, such as a 15.9% increase in sequence average accuracy. This provides compelling evidence that our training strategy is crucial, transforming the tools from a potential distraction into a potent performance amplifier.

4.3. Ablation Study

4.3.1. Ablation on Progressive Training Strategy

To validate the effectiveness of our proposed three-stage progressive training strategy, we conduct a series of detailed ablation studies. As shown in Table 2, we compare the performance of model variants under different combinations of training stages. Each variant is evaluated under three dis-

tinct modes: forced text-only reasoning ($\mathcal{M}_{\text{text}}$), forced tool-assisted reasoning ($\mathcal{M}_{\text{tool}}$), and a free-choice mode where the agent can select its own reasoning pathway ($\mathcal{M}_{\text{free}}$). The comparisons in Table 2 lead to the following conclusions.

RL is Key to Performance. The results unequivocally demonstrate that RL is essential for unlocking the agent’s capabilities. All variants trained with RL substantially outperform the SFT-only baseline (Variant-1) across all metrics. For instance, in the free-choice setting, the SFT-only model achieves just 25.41% joint accuracy, while all RL-trained variants surpass 51%.

FCM-RL Sharpens Execution, AMS-RL Hones Selection. Our ablations reveal a clear trade-off between the two RL stages. Variant-2 excels in forced-mode execution, achieving the highest accuracy in the $\mathcal{M}_{\text{text}}$ mode among the variants. Conversely, Variant-3 develops better mode-selection intelligence, reflected by a higher MSA score (55.40% vs. 52.87%). This shows that FCM-RL is crucial for strengthening individual reasoning pathways, while AMS-RL is vital for teaching the agent when to use them.

Full Progressive Strategy Achieves Optimal Performance. Our complete three-stage strategy allows *DriveAgent-RL* to achieve the best overall results, outperforming all other variants across every metric. Our final model not only masters unimodal execution but also develops superior mode-selection accuracy (65.93% MSA) via AMS-RL. This synergy validates our progressive “foundation \rightarrow strengthening \rightarrow selectio” approach, which improves both the agent’s individual skills and its intelligence to deploy them adaptively.

Table 2. **Ablation on the progressive training strategy.** We evaluate different combinations of our three training stages: Dual-Mode SFT (DM-SFT), Forced-Contrastive Mode RL (FCM-RL), and Adaptive Mode-Selection RL (AMS-RL). Performance is reported across three evaluation modes: forced tool-use ($\mathcal{M}_{\text{tool}}$), forced text-only ($\mathcal{M}_{\text{text}}$), and free-choice ($\mathcal{M}_{\text{free}}$). Best results in each column are in **bold**.

Variant	Training Stage			First Frame-Joint ACC (%) \uparrow			Sequence Avg-Joint ACC (%) \uparrow			MSA (%) \uparrow
	DM-SFT	FCM-RL	AMS-RL	$\mathcal{M}_{\text{tool}}$	$\mathcal{M}_{\text{text}}$	$\mathcal{M}_{\text{free}}$	$\mathcal{M}_{\text{tool}}$	$\mathcal{M}_{\text{text}}$	$\mathcal{M}_{\text{free}}$	
Variant-1	✓			39.55	18.49	25.41	35.53	23.88	27.25	41.00
Variant-2	✓	✓		66.07	46.10	53.64	41.24	31.49	35.93	52.87
Variant-3	✓		✓	61.35	37.92	51.22	40.44	30.65	36.89	55.40
DriveAgent-R1 (Ours)	✓	✓	✓	71.23	61.42	70.11	43.20	38.03	44.06	65.93

Table 3. **Ablation on visual input.** We compare performance with and without visual input. The performance drop (%) when images are removed is shown in parentheses.

Model	Inference Setting	First Frame-Joint ACC	Seq. Avg-Joint ACC
Trained w/o tools	w/ image	44.34	32.81
	w/o image	33.84 (-23.7%)	29.19 (-11.0%)
DriveAgent-R1 (Ours)	w/ image	70.11	44.06
	w/o image	39.90 (-43.1%)	34.72 (-21.2%)

4.3.2. Active Perception Amplifies Visual Dependency

To verify that our model’s decisions are visually grounded, we conduct an ablation study by removing all image inputs during inference. To isolate the impact of active perception, we compare *DriveAgent-R1* against a carefully designed baseline. This baseline is trained on the identical data samples and undergoes the SFT and RL pipeline, but with one critical difference: the vision toolkit is never introduced during its training. We refer to this as the “Trained w/o tools” variant. As shown in Table 3, the results are revealing:

DriveAgent-R1 is Genuinely Vision-Driven. Withholding visual information causes a catastrophic performance drop for DriveAgent-R1, with its first-frame joint accuracy plummeting by 43.1%. This substantial degradation strongly validates that our agent’s decisions are genuinely driven by what it sees, rather than by exploiting textual shortcuts from navigation or speed commands.

Active Perception is Key to Deep Visual Reliance. Crucially, the “Trained w/o tools” variant experiences a much smaller performance drop (23.7% vs. 43.1%). This comparison demonstrates that without the ability to actively probe the environment with tools, an agent’s capacity to leverage visual information is inherently limited. It is therefore our active perception mechanism that fosters a deep and meaningful reliance on visual reality, making *DriveAgent-R1* more robust and its decisions more grounded.

5. Conclusion

In this work, we introduced *DriveAgent-R1*, an advanced autonomous driving agent that addresses critical challenges in long-horizon, high-level behavioral decision-making. We

presented two core innovations: an active perception mechanism, realized through a versatile vision toolkit, and a hybrid-thinking framework that allows the agent to dynamically switch between efficient text-based and deliberate tool-based reasoning. To cultivate these capabilities, we designed a novel, three-stage progressive training strategy centered on RL. Our extensive experiments demonstrate that *DriveAgent-R1* achieves state-of-the-art performance despite its lightweight size, and our ablations confirm that its decisions are genuinely grounded in the visual evidence it actively perceives. By reasoning and perceiving more like a human driver, *DriveAgent-R1* enhances not only the interpretability of its decisions but also, ultimately, the safety of its operation.

Despite these promising results, our work points to several exciting avenues for future research. The current vision toolkit could be expanded to include a more diverse set of tools to handle an even wider range of complex scenarios. Furthermore, a significant future direction is to adapt our hybrid-thinking and active-perception framework to the task of direct, low-level trajectory generation, bridging the gap between high-level semantic intent and precise motion control.

References

- [1] Anthropic. Introducing Claude 4. <https://www.anthropic.com/news/claude-4>, 2025. Accessed: 2025-07-27. 9
- [2] Shuai Bai, Keqin Chen, Xuejing Liu, Jialin Wang, Wenbin Ge, Sibao Song, Kai Dang, Peng Wang, Shijie Wang, Jun Tang, Humen Zhong, Yanzhi Zhu, Mingkun Yang, Zhaohai Li, Jianqiang Wan, Pengfei Wang, Wei Ding, Zheren Fu, Yiheng

- Xu, Jiabo Ye, Xi Zhang, Tianbao Xie, Zesen Cheng, Hang Zhang, Zhibo Yang, Haiyang Xu, and Junyang Lin. Qwen2.5-vl technical report. *arXiv preprint arXiv:2502.13923*, 2025. 4, 8, 9
- [3] Yoshua Bengio, Jérôme Louradour, Ronan Collobert, and Jason Weston. Curriculum learning. In *Proceedings of the 26th annual international conference on machine learning*, 2009. 7, 13
- [4] ByteDance. Seed-1.6. https://seed.bytedance.com/zh/seed1_6, 2024. Accessed: 2025-07-27. 9
- [5] Zihui Cheng, Qiguang Chen, Xiao Xu, Jiaqi Wang, Weiyun Wang, Hao Fei, Yidong Wang, Alex Jinpeng Wang, Zhi Chen, Wanxiang Che, and Libo Qin. Visual thoughts: A unified perspective of understanding multimodal chain-of-thought, 2025. 2, 3
- [6] Tushar Choudhary, Vikrant Dewangan, Shivam Chandhok, Shubham Priyadarshan, Anushka Jain, Arun K Singh, Siddharth Srivastava, Krishna Murthy Jatavallabhula, and K Madhava Krishna. Talk2bev: Language-enhanced bird’s-eye view maps for autonomous driving. In *2024 IEEE International Conference on Robotics and Automation (ICRA)*. IEEE, 2024. 3
- [7] Zheng Chu, Jingchang Chen, Qianglong Chen, Weijiang Yu, Tao He, Haotian Wang, Weihua Peng, Ming Liu, Bing Qin, and Ting Liu. Navigate through enigmatic labyrinth a survey of chain of thought reasoning: Advances, frontiers and future. In *Proceedings of the 62nd Annual Meeting of the Association for Computational Linguistics*, 2024. 3
- [8] Gheorghe Comanici, Eric Bieber, Mike Schaekermann, Ice Pasupat, Naveen Sachdeva, Inderjit Dhillon, Marcel Blistein, Ori Ram, Dan Zhang, Evan Rosen, et al. Gemini 2.5: Pushing the frontier with advanced reasoning, multimodality, long context, and next generation agentic capabilities. *arXiv preprint arXiv:2507.06261*, 2025. 9
- [9] Liqi He, Zuchao Li, Xiantao Cai, and Ping Wang. Multimodal latent space learning for chain-of-thought reasoning in language models. In *Proceedings of the AAAI conference on artificial intelligence*, 2024. 3
- [10] Yihan Hu, Jiazhi Yang, Li Chen, Keyu Li, Chonghao Sima, Xizhou Zhu, Siqi Chai, Senyao Du, Tianwei Lin, Wenhui Wang, et al. Planning-oriented autonomous driving. In *Proceedings of the IEEE/CVF conference on computer vision and pattern recognition*, 2023. 1
- [11] Yushi Hu, Weijia Shi, Xingyu Fu, Dan Roth, Mari Ostendorf, Luke Zettlemoyer, Noah A Smith, and Ranjay Krishna. Visual sketchpad: Sketching as a visual chain of thought for multimodal language models. In *Advances in Neural Information Processing Systems*, 2024. 2, 3
- [12] Bo Jiang, Shaoyu Chen, Qing Xu, Bencheng Liao, Jiajie Chen, Helong Zhou, Qian Zhang, Wenyu Liu, Chang Huang, and Xinggang Wang. Vad: Vectorized scene representation for efficient autonomous driving. *ICCV*, 2023. 1
- [13] Bo Jiang, Shaoyu Chen, Qian Zhang, Wenyu Liu, and Xinggang Wang. Alphadrive: Unleashing the power of vlms in autonomous driving via reinforcement learning and reasoning, 2025. 2, 3, 7
- [14] Lingjie Jiang, Xun Wu, Shaohan Huang, Qingxiu Dong, Zewen Chi, Li Dong, Xingxing Zhang, Tengchao Lv, Lei Cui, and Furu Wei. Think only when you need with large hybrid-reasoning models, 2025. 8
- [15] Chengzu Li, Wenshan Wu, Huanyu Zhang, Yan Xia, Shaoguang Mao, Li Dong, Ivan Vulić, and Furu Wei. Imagine while reasoning in space: Multimodal visualization-of-thought. *arXiv preprint arXiv:2501.07542*, 2025. 2, 3
- [16] Hongyu Li, Jinyu Chen, Ziyu Wei, Shaofei Huang, Tianrui Hui, Jialin Gao, Xiaoming Wei, and Si Liu. Llava-st: A multimodal large language model for fine-grained spatial-temporal understanding. In *Proceedings of the Computer Vision and Pattern Recognition Conference*, 2025. 3
- [17] Yue Li, Meng Tian, Dechang Zhu, Jiangtong Zhu, Zhenyu Lin, Zhiwei Xiong, and Xinhai Zhao. Drive-r1: Bridging reasoning and planning in vlms for autonomous driving with reinforcement learning, 2025. 2, 3
- [18] Ziyu Liu, Zeyi Sun, Yuhang Zang, Xiaoyi Dong, Yuhang Cao, Haodong Duan, Dahua Lin, and Jiaqi Wang. Visual-rft: Visual reinforcement fine-tuning. *arXiv preprint arXiv:2503.01785*, 2025. 3, 7
- [19] Jieyi Long. Large language model guided tree-of-thought. *arXiv preprint arXiv:2305.08291*, 2023. 3
- [20] Jiageng Mao, Yuxi Qian, Junjie Ye, Hang Zhao, and Yue Wang. Gpt-driver: Learning to drive with gpt. *arXiv preprint arXiv:2310.01415*, 2023. 3
- [21] Fanxu Meng, Haotong Yang, Yiding Wang, and Muhan Zhang. Chain of images for intuitively reasoning. *arXiv preprint arXiv:2311.09241*, 2023. 3
- [22] Debjyoti Mondal, Suraj Modi, Subhadarshi Panda, Rituraj Singh, and Godawari Sudhakar Rao. Kam-cot: Knowledge augmented multimodal chain-of-thoughts reasoning. In *Proceedings of the AAAI conference on artificial intelligence*, 2024. 3
- [23] Ming Nie, Renyuan Peng, Chunwei Wang, Xinyue Cai, Jianhua Han, Hang Xu, and Li Zhang. Reason2drive: Towards interpretable and chain-based reasoning for autonomous driving. In *European Conference on Computer Vision*. Springer, 2024. 3
- [24] OpenAI. GPT-4.1. Technical report, OpenAI, 2024. Accessed: 2025-07-27. 9
- [25] OpenAI. Introducing O3 and O4 mini. <https://openai.com/index/introducing-o3-and-o4-mini/>, 2025. Accessed: 2025-07-24. 2, 3
- [26] Pranjal Paul, Anant Garg, Tushar Choudhary, Arun Kumar Singh, and K Madhava Krishna. Lego-drive: Language-enhanced goal-oriented closed-loop end-to-end autonomous driving. In *2024 IEEE/RSJ International Conference on Intelligent Robots and Systems (IROS)*. IEEE, 2024. 1
- [27] Kangan Qian, Sicong Jiang, Yang Zhong, Ziang Luo, Zilin Huang, Tianze Zhu, Kun Jiang, Mengmeng Yang, Zheng Fu, Jinyu Miao, Yining Shi, He Zhe Lim, Li Liu, Tianbao Zhou, Huang Yu, Yifei Hu, Guang Li, Guang Chen, Hao Ye, Lijun Sun, and Diange Yang. Agentthink: A unified framework for tool-augmented chain-of-thought reasoning in vision-language models for autonomous driving, 2025. 2, 3
- [28] Hao Shao, Yuxuan Hu, Letian Wang, Guanglu Song, Steven L Waslander, Yu Liu, and Hongsheng Li. Lmdrive: Closed-loop

- end-to-end driving with large language models. In *Proceedings of the IEEE/CVF Conference on Computer Vision and Pattern Recognition*, 2024. 3
- [29] Zhihong Shao, Peiyi Wang, Qihao Zhu, Runxin Xu, Junxiao Song, Mingchuan Zhang, Y.K. Li, Y. Wu, and Daya Guo. Deepseekmath: Pushing the limits of mathematical reasoning in open language models, 2024. 3, 7
- [30] Chonghao Sima, Katrin Renz, Kashyap Chitta, Li Chen, Hanxue Zhang, Chengen Xie, Jens Beißwenger, Ping Luo, Andreas Geiger, and Hongyang Li. Drivelm: Driving with graph visual question answering. In *European conference on computer vision*, 2024. 1, 3
- [31] Christoph Stiller, Matthias Althoff, Christoph Burger, Barbara Deml, Lutz Eckstein, and Frank Flemisch. *Cooperatively Interacting Vehicles: Methods and Effects of Automated Cooperation in Traffic*. Springer Nature, 2024. 1
- [32] Alex Su, Haozhe Wang, Weiming Ren, Fangzhen Lin, and Wenhui Chen. Pixel reasoner: Incentivizing pixel-space reasoning with curiosity-driven reinforcement learning. *arXiv preprint arXiv:2505.15966*, 2025. 3, 7
- [33] Md Arafat Sultan, Jatin Ganhotra, and Ramón Fernández Astudillo. Structured chain-of-thought prompting for few-shot generation of content-grounded qa conversations. *arXiv preprint arXiv:2402.11770*, 2024. 3
- [34] Xiaoyu Tian, Junru Gu, Bailin Li, Yicheng Liu, Zhiyong Zhao, Yang Wang, Kun Zhan, Peng Jia, Xianpeng Lang, and Hang Zhao. Drivevlm: The convergence of autonomous driving and large vision-language models. *arXiv preprint arXiv:2402.12289*, 2024. 1, 2, 3, 8
- [35] Letian Wang, Yeping Hu, Liting Sun, Wei Zhan, Masayoshi Tomizuka, and Changliu Liu. Transferable and adaptable driving behavior prediction. *arXiv preprint arXiv:2202.05140*, 2022. 1
- [36] Lei Wang, Yi Hu, Jiabang He, Xing Xu, Ning Liu, Hui Liu, and Heng Tao Shen. T-sciq: Teaching multimodal chain-of-thought reasoning via large language model signals for science question answering. In *Proceedings of the AAAI Conference on Artificial Intelligence*, 2024. 3
- [37] Xuezhi Wang and Denny Zhou. Chain-of-thought reasoning without prompting. *Advances in Neural Information Processing Systems*, 2024. 3
- [38] Yuping Wang, Shuo Xing, Cui Can, Renjie Li, Hongyuan Hua, Kexin Tian, Zhaobin Mo, Xiangbo Gao, Keshu Wu, Sulong Zhou, et al. Generative ai for autonomous driving: Frontiers and opportunities. *arXiv preprint arXiv:2505.08854*, 2025. 1
- [39] Jason Wei, Xuezhi Wang, Dale Schuurmans, Maarten Bosma, Fei Xia, Ed Chi, Quoc V Le, Denny Zhou, et al. Chain-of-thought prompting elicits reasoning in large language models. *Advances in neural information processing systems*, 2022. 3
- [40] Guowei Xu, Peng Jin, Hao Li, Yibing Song, Lichao Sun, and Li Yuan. Llava-cot: Let vision language models reason step-by-step, 2024. 2, 3
- [41] Zhenhua Xu, Yujia Zhang, Enze Xie, Zhen Zhao, Yong Guo, Kwan-Yee K. Wong, Zhenguo Li, and Hengshuang Zhao. Drivegpt4: Interpretable end-to-end autonomous driving via large language model. *IEEE Robotics and Automation Letters*, 2024. 1, 2
- [42] Lihe Yang, Bingyi Kang, Zilong Huang, Zhen Zhao, Xianggang Xu, Jiashi Feng, and Hengshuang Zhao. Depth anything v2. *Advances in Neural Information Processing Systems*, 2024. 5
- [43] Hanxue Zhang, Haoran Jiang, Qingsong Yao, Yanan Sun, Renrui Zhang, Hao Zhao, Hongyang Li, Hongzi Zhu, and Zetong Yang. Detect anything 3d in the wild. In *IEEE International Conference on Computer Vision*, 2025. 5
- [44] Kesen Zhao, Beier Zhu, Qianru Sun, and Hanwang Zhang. Unsupervised visual chain-of-thought reasoning via preference optimization, 2025. 3
- [45] Ziwei Zheng, Michael Yang, Jack Hong, Chenxiao Zhao, Guohai Xu, Le Yang, Chao Shen, and Xing Yu. Deepeyes: Incentivizing” thinking with images” via reinforcement learning. *arXiv preprint arXiv:2505.14362*, 2025. 3, 7

A. Appendix Section

A.1. Call Format of Tools

```
<tool_call>
  <tool_name>Retrieve High-Resolution
  View</tool_name>
  <params>{"frame_index": "-1s", "
  view_index": "front_left"}</params>
</tool_call>
```

Call Format of Retrieve High-Resolution View

```
<tool_call>
  <tool_name>Depth Estimation</tool_name>
  <params>{"view_index": "front"}</params>
  >
</tool_call>
```

Call Format of Depth Estimation

```
<tool_call>
  <tool_name>RoI Inspection</tool_name>
  <params>{"view_index": "front_left", "
  area": [x_min, y_min, x_max, y_max], "
  label": "the traffic lights"}</params>
</tool_call>
```

Call Format of RoI Inspection

```
<tool_call>
  <tool_name>3D Object Detection</
  tool_name>
  <params>{"view_index": "front", "
  object_text": "barrier"}</params>
</tool_call>
```

Call Format of 3D Object Detection

A.2. Reward Design Details

Accuracy Reward (R_{acc})

Our accuracy reward, R_{acc} , evaluates the quality of the predicted meta-action sequence by separately assessing its speed (Y_{speed}) and trajectory (Y_{traj}) components. The total reward is a weighted average of the similarity scores from these two components:

$$R_{acc} = w_{speed} \cdot \text{Sim}(Y_{speed}, \hat{Y}_{speed}) + w_{traj} \cdot \text{Sim}(Y_{traj}, \hat{Y}_{traj})$$

To account for the inherent diversity of reasonable driving decisions, where the ground truth represents only one of several valid possibilities, we design a robust similarity function, $\text{Sim}(Y, \hat{Y})$. This function considers both strict and trend-based matching between a predicted sequence \hat{Y} and a ground-truth sequence Y to provide a more holistic evaluation. It is defined as the maximum of a strict similarity score (S_{strict}) and a trend similarity score (S_{trend}):

$$\text{Sim}(Y, \hat{Y}) = \max(S_{strict}(Y, \hat{Y}), S_{trend}(Y, \hat{Y}))$$

- **Strict Similarity (S_{strict})** We use the standard normalized Levenshtein distance to compute the similarity between the predicted sequence \hat{Y} and the ground-truth sequence Y :

$$S_{strict}(Y, \hat{Y}) = 1 - \frac{D_{edit}(Y, \hat{Y})}{\max(|Y|, |\hat{Y}|)}$$

- **Trend Similarity (S_{trend})**: To evaluate action trends while being robust to minor variations in duration, we introduce a similarity metric based on Run-Length Encoding (RLE). This method first compresses a sequence by representing consecutive identical actions as a single (action, count) pair. For instance, the sequence $Y = (a, a, b)$ is transformed into its RLE representation, $\text{RLE}(Y) = ((a, 2), (b, 1))$. A weighted edit distance is then computed on these compressed sequences.

$$S_{trend}(Y, \hat{Y}) = S_{strict}(\text{RLE}(Y), \text{RLE}(\hat{Y}))$$

When calculating the matching cost between two compressed elements (a, c) and (\hat{a}, \hat{c}) , we consider both the action type and the duration count:

$$\text{Similarity}_{\text{element}} = \mathbb{I}(\hat{a} = a) \cdot \left(1 - \alpha \frac{|\hat{c} - c|}{\hat{c} + c}\right)$$

Format Consistency Reward (R_{fmt})

This reward ensures the agent's outputs adhere to our specified framework. It is a rule-based score that assesses compliance with the preset structured format (e.g., using correct tags to enclose thought processes) and, more critically, penalizes action-declaration inconsistency. Specifically, it discourages invoking tools within the \mathcal{M}_{text} mode or failing to do so within the \mathcal{M}_{tool} mode. This forces the agent to learn and respect the distinct boundaries of each thinking mode, establishing a solid foundation for the subsequent adaptive selection stage.

Tool Usage Reward (R_{tool})

The Tool Usage Reward (R_{tool}) is designed to encourage the agent to use tools not just frequently, but effectively. Its core principle is to link the reward for tool usage directly to the final outcome quality, measured by the accuracy reward R_{acc} . To achieve this in a progressive manner that balances exploration and exploitation, we employ a dynamic reward window based on curriculum learning [3]. This reward is only applied when the agent autonomously selects the `<think_tool>` mode.

Dynamic Reward Window

Instead of a single threshold, we define a dynamic reward window for the accuracy score, which is composed of a lower bound $\theta_{lower(s)}$ and an upper bound $\theta_{upper(s)}$, where s is the current training step. Both bounds increase linearly throughout the training process to gradually raise the performance expectation for what constitutes effective tool use.

The bounds are calculated as follows:

$$\theta_{\text{bound}}(\mathbf{s}) = \theta_{\text{start}} + (\theta_{\text{end}} - \theta_{\text{start}}) \cdot \min \left(1, \frac{\mathbf{s} - \mathbf{s}_{\text{start}}}{\mathbf{s}_{\text{end}} - \mathbf{s}_{\text{start}}} \right)$$

The final R_{tool} for a given trajectory is calculated using a piecewise function based on its accuracy reward R_{acc} relative to the dynamic window at step \mathbf{s} :

$$R_{\text{tool}}(\mathbf{s}) = \begin{cases} R_{\text{penalty}} & \text{if } R_{\text{acc}} < \theta_{\text{lower}}(\mathbf{s}) \\ R_{\text{interp}}(\mathbf{s}) & \text{if } \theta_{\text{lower}}(\mathbf{s}) \leq R_{\text{acc}} \leq \theta_{\text{upper}}(\mathbf{s}) \\ R_{\text{bonus}} \cdot R_{\text{base tool}} & \text{if } R_{\text{acc}} > \theta_{\text{upper}}(\mathbf{s}) \end{cases} \quad (1)$$

The components are defined as:

- **Penalty Zone:** If the accuracy is below the lower bound, the agent receives a constant negative reward R_{penalty} , discouraging clearly ineffective tool use.
- **Bonus Zone:** If the accuracy surpasses the upper bound, the agent receives a constant positive reward R_{bonus} , scaled by the average base quality of the tool calls ($R_{\text{base tool}}$). This reinforces highly successful tool-driven reasoning.
- **Buffer Zone:** If the accuracy falls within the window, which acts as a buffer, the reward is linearly interpolated between the penalty and the full bonus. This provides a smooth gradient for improvement. The interpolated reward $R_{\text{interp}}(\mathbf{s})$ is calculated as:

$$R_{\text{interp}}(\mathbf{s}) = R_{\text{penalty}} + (R_{\text{bonus}} \cdot R_{\text{base tool}} - R_{\text{penalty}}) \cdot \frac{R_{\text{acc}} - \theta_{\text{lower}}(\mathbf{s})}{\theta_{\text{upper}}(\mathbf{s}) - \theta_{\text{lower}}(\mathbf{s})} \quad (2)$$

The term $R_{\text{base tool}}$ represents the average compliance of all tool calls within the trajectory, assessing the correctness of tool names, parameters, and successful execution.

This formulation creates a curriculum where the agent is initially encouraged to explore the utility of tools with a lenient reward landscape, and is later pushed to refine its strategy to only invoke tools when they lead to high-quality, precise outcomes.